POLITECNICO DI TORINO
Repository ISTITUZIONALE

Accelerating fusion energy industrialisation through process standardisation

Original
Accelerating fusion energy industrialisation through process standardisation / Centomani, G.V., Iaboni, A., Avella, D., Buonocore, A., Barone, L., Cederle, L., De Bastiani, M., Durastanti, R., Ferrero, G., Forte, R., Gallo, E., Indrigo, D., Meschini, S., Pettinari, D., Podenzani, F., Romano, M., Salvato, D., Testoni, R., Zucchetti, M., Spagnuolo, G.A.. - In: FUSION ENGINEERING AND DESIGN. - ISSN 0920-3796. - ELETTRONICO. - 231:(2026). [10.1016/j.fusengdes.2026.115878]

Availability:
This version is available at: 11583/3014592 since: 2026-08-18T15:08:42Z

Publisher:
Elsevier

Published
DOI:10.1016/j.fusengdes.2026.115878

Terms of use:

This article is made available under terms and conditions as specified in the corresponding bibliographic description in the repository

Publisher copyright

(Article begins on next page)

29 November 2026

Fusion Engineering and Design 231 (2026) 115878

Contents lists available at ScienceDirect

Fusion Engineering and Design

journal homepage: www.elsevier.com/locate/fusengdes

Accelerating fusion energy industrialisation through process standardisation

G.V. Centomani [a,*], A. Iaboni [a], D. Avella [b], A. Buonocore [b], L. Barone [a], L. Cederle [a], M. De Bastiani [b], R. Durastanti [b], G. Ferrero [c], R. Forte [b], E. Gallo [a], D. Indrigo [b], S. Meschini [c], D. Pettinari [c], F. Podenzani [a], M. Romano [a], D. Salvato [b], R. Testoni [c], M. Zucchetti [c], G.A. Spagnuolo [a]

[a] Eni SpA, piazzale Enrico Mattei 1, 00144, Roma, Italy
[b] EniProgetti S.p.A., Via Felice Maritano 26, 20097 San Donato Milanese, Italy
[c] Dipartimento Energia, Politecnico di Torino, c.so Duca degli Abruzzi 24, 10129 Torino, Italy

ARTICLE INFO

Keywords:
System engineering
Industrial procedures
Nuclear standards
Breeding blanket
Fuel cycle

ABSTRACT

In the path towards the exploitation of nuclear fusion as a virtually unlimited, reliable, and carbon-free energy source, demonstrating tritium self-sufficiency and achieving competitive net electricity production for the grid are of paramount importance.

As Eni fosters the industrialisation of magnetic confinement fusion, we are committed to mitigating risks and accelerating the development of fusion power plants. To this end, we apply consolidated engineering methodologies and structured risk management strategies from the earliest stages of the design process. This approach leverages our extensive expertise in engineering and project management, built over decades of experience in complex energy infrastructure projects.

This contribution presents two case studies that exemplify Eni's approach to bridging conventional engineering practices with the unique challenges of fusion systems engineering. The focus is placed on the Breeding Blanket (BB) and Tritium Fuel Cycle (TFC) systems, both of which are pivotal for the availability and operability of future fusion power plants.

A generic Fusion Power Plant (FPP) configuration has been adopted as the reference framework for this study.

The application of the proposed approach to these systems provides concrete technical insights into its effectiveness. For the Breeding Blanket, integrated multi-physics parametric analyses enable the identification of feasible design envelopes capable of achieving tritium breeding ratios above unity while satisfying thermal and structural constraints. For the Tritium Fuel Cycle, the structured process-design approach supports the definition and preliminary sizing of key subsystems and enables early assessment of tritium inventory in the plant.

These results also underscore the importance of early-stage standardisation in enhancing design transparency and reinforcing system integration within the overall plant architecture. Overall, the proposed approach can significantly streamline the design process and facilitate the transition from experimental devices to commercially viable fusion power plants, while supporting effective engagement with regulators and industrial stakeholders.

1. Introduction

Complex systems, such as future Fusion Power Plants (FPP), would benefit from the combination of systems engineering principles with standardized engineering procedures to guide technologies from research toward industrial deployment. The motivation of this work is to show how such an integrated framework can support fusion plant design from the earliest stages by ensuring consistency in design methodology, quality assurance, and risk management across all development phases.

The Breeding Blanket (BB) and Tritium Fuel Cycle (TFC) are selected as complementary case studies because they represent two critical, yet substantially different, systems for ensuring the availability and

* Corresponding author.
E-mail address: giuliavaleria.centomani@eni.com (G.V. Centomani).

https://doi.org/10.1016/j.fusengdes.2026.115878
Received 30 January 2026; Received in revised form 9 June 2026; Accepted 9 June 2026
Available online 7 July 2026
0920-3796/© 2026 Published by Elsevier B.V.

operability of future FPPs. The BB is primarily driven by multi-physics constraints, including neutronic performance, thermal-hydraulic behaviour, structural integrity, and material compatibility, and is strongly coupled to the overall reactor architecture and design as an essential system directly involved in tritium breeding, shielding, and heat extraction. Conversely, the TFC shares several features with chemical process plants and is mainly governed by process design, safety and radiation protection requirements, tritium inventory control, and the integration of multiple interconnected subsystems, each performing a dedicated function. Considering both systems therefore allows the proposed methodology to be tested not only on a component-oriented system, but also on a process-oriented system.

Both areas stand to benefit from know-how and technology transfer, as well as from early-stage process standardisation rooted in Eni's industrial background. These systems are used here as test cases to demonstrate how the proposed approach can improve traceability of design decisions, facilitate integration with the overall plant architecture, and provide a clearer basis for engagement with regulators and industrial stakeholders.

1.1. Industrial approach in fusion engineering

The global fusion program is going through a big change from custom-built experimental devices to standardised, industrial power-producing systems. The needs of Demonstration Power Plants (DEMO) and Fusion Pilot Plants (FPPs) are causing this big change. Indeed, these plants need to be able to run reliably, be able to get a license under the relevant rules, and be able to compete with other plants on price. The BB and the TFC are among the most important parts of this change. Together, they decide how safe, efficient, and available the plant is [1, 2].

Systems engineering, nuclear-grade design codes, and industrial manufacturing standards (i.e. most notably RCC-MRx, ASME BPVC Section XI Division 2, and new ISO fusion standards) are being used to formalise the BB and TFC design processes [3–9]. A dedicated effort is also ongoing to develop the ASME BPVC Section III - Rules for Construction of Nuclear Facility Components - Division 4 - Fusion Energy Devices [10]. However, no formalisation of the design analysis process has already been completed.

Industrialisation is undoubtedly made possible by the Systems Engineering (SE) approach to managing reactor complexity, which involves tens of different systems. In fact, SE ensures consistency between plant-level goals and component-level design by breaking down and tracing stakeholders, safety, and regulatory requirements through hierarchical document structures. Given the limited operational experience with fusion materials and configurations, functional architectures allow solution-agnostic exploration before hardware commitment, which is crucial. System-level codes are also essential in supporting design exploration activities by accelerating the sequence of design and analysis activities when generating a design configuration [9]. Additionally, the parallel industrial development of BB and TFC subsystems is made possible by the formalisation of interfaces using Interface Control Documents (ICDs), Interface Definition Documents (IDDs), and Interface Requirements (IRs) [11,12].

The shift from custom laboratory components to modular, repeatable designs has been enforced by efforts to standardise through Design for Manufacture. As an illustration, the EU-DEMO's switch from Multi-Module Segments (MMS), where each European breeding blanket concept was conceived differently from each other, to Single Module Segments (SMS) greatly decreased pipe penetrations, welds, and failure points, enhancing dependability and remote maintainability and reducing the variety of configurations with respect to the interfacing systems, [13]. Other examples are related to the large-scale production and qualification of industrial fabrication technologies like Additive Manufacturing (AM) for complex internal cooling geometries, Laser Beam Welding (LBW) and Electron Beam Welding (EBW) for low-distortion joining, and Hot Isostatic Pressing (HIP) for diffusion bonding of RAFM steel plates [14–16]. For example, China's CFETR program has already established group standards for weld inspection and demonstrated batch production of RAFM steel components, which is a major step toward global supply chain maturity [17].

The transition from batch-wise experimental processing to continuous, high-throughput systems overseen by strict nuclear regulatory frameworks is currently driving efforts to industrialise and standardise the fusion TFC. The following are a few instances of the regulatory frameworks connected to the primary fuel cycle systems:

- ISO Fusion Standards: A critical milestone is ISO 16,646:2024 [18], which establishes standards for the construction and functioning of ventilation and confinement systems for fuel handling and tritium fusion facilities. For "high tritium inventories," which are defined as those weighing >10–100 *g*, it sets safety standards. Additionally, ISO/DIS 19,991 [19] is under development to standardize Supersonic Molecular Beam Injection (SMBI) fueling techniques.
- Nuclear Design Codes: The RCC-MRx (2022 edition) [3,4] has been updated with a dedicated Volume I specifically for components operating under vacuum, alongside refined rules for irradiated components near neutron sources. On the other side, the ASME BPVC Section XI Division 2 [20] offers the Reliability and Integrity Management (RIM) program, a technology-neutral framework that uses probabilistic risk assessment (PRA) to determine component-level requirements from plant-level safety targets.

Significant efforts have also been made to map and scale industrial technology. In this regard, a thorough study conducted in 2025 by EUROfusion and Fusion for Energy (F4E) identified 48 crucial technologies in four domains [21] (i.e. fueling and storage, pumping, membranes and packing, and tritium management) to identify the supply chain and prioritise R&D for commercial viability.

Moreover, the development of significant test facilities for the system's industrial scale-up has also received special attention. In this context, it is important to note that the main industrial testbed for closed-loop tritium accounting and processing will be the UKAEA-Eni H3AT facility, which is anticipated to be the largest TFC facility in the world by 2028. Other examples include Kyoto Fusioneering's UNITY1 [22] and UNITY2 [23], which are being built to demonstrate respectively technological solutions for breeder-related components and fuel cycle technologies.

In this frame, what appears missing is the identification and standardisation of the industrial methodologies for the design of those systems. For this reason, Eni is using cross-sectoral engineering techniques. Mature engineering techniques, standardised process models, and structured workflows are all systematically adopted in this industrial approach to FPP design and are presented in the following.

As maturity increases, established models and procedures offer an organised series of stages, decision points, and verification tasks that aid in managing uncertainty, controlling technical risk, and gradually consolidating design definitions. This method guarantees that design, testing, and qualification activities are in line with well-defined industrialisation targets and supports transparent go/no-go decisions when combined with technology assessment and market scouting analyses.

Vulnerabilities in the supply chain can also be found using this method. This will help to reduce the investments that are estimated to be in the order of hundreds of millions of euros over the next ten years if these gaps are not closed early. In the following chapters, a description and application of the industrial methodologies for the design of BB and TFC systems is reported.

2. Application to breeding blanket design

To define and stardardise the design process of systems like the BB, it is important to identify the main functions. Indeed, the BB is the system

responsible for (i) ensuring the tritium self-sufficiency of the power plant by tritium breeding via $^{6}Li(n,t)^{4}He$ and $^{7}Li(n,n't)^{4}He$ reactions, which convert neutrons into tritium (ii) slowing down and capturing neutrons and transferring the heat at relevant conditions for electricity production purposes and (iii) shielding the superconducting coils from neutron bombardment.

From the analyses of BB functions, it is clear that different physics are involved since the early design phase. For instance, neutronic analyses are needed to estimate the tritium production rates, the power density deposition, as well as the material activation and the damage due to the neutron bombardment. On the other hand, thermal-hydraulic analyses are necessary to determine the material and fluid temperatures, and thus to verify that heat is transferred under relevant conditions for electricity production while maintaining the structural integrity. Lastly, the thermo-mechanical studies demonstrate that the BB withstand the given loads and is compliant with the prescriptions of Codes&Standards. Furthermore, all these analyses contribute to the definition of the technical specification for manufacturing and installation, providing the nuclear manufacturer with all the evidence required by the regulator for the licensing of this system.

Therefore, it is evident that these analyses and the design process become extremely important for the realisation and industrialisation of fusion technology and, particularly, of BB.

So far, the scientific community has produced several BB design concepts (for instance, in [1,24–27]) and proposed customised approaches to the design (some examples can be found in [28–30]). Of course, there is a common thread among them (i.e. neutronic → thermal-hydraulic → thermo-mechanical analyses) as well as the attempt to uniformise the approach to the design. However, no complete formalisation and standardisation has been pursued until now.

The approach, herewith proposed, aims at the creation of an agreed and standardised design process that can ease the industrialisation of BB systems [31]. The approach starts with the investigation of different design solutions according to the different physics involved (e.g. neutronics, thermal-hydraulics, thermo-mechanics) as well as the different requirements. This first step is done through several parametric studies according to the physics and requirements. Subsequently, the solutions, identified for the single problems, are integrated into a unique CAD considering the manufacturability and assembly of BB. Finally, the integrated design is investigated, and the overall performances checked against requirements. This approach allows the early identification of weak points and the possibility to introduce dedicated solutions. Furthermore, it is possible to decompose the complex BB design into simpler technical issues (e.g. heat flux on the first-wall, FW, or in the divertor zone) that are then recomposed to create the integrated BB design. Moreover, this approach introduces from the beginning some considerations about the manufacturing and assembly of the BB system, avoiding the development of a design solution that is difficult to build. A simplified workflow illustrating this iterative process is presented in Fig. 1.

In the following chapters, the workflow has been applied, as an example, on the BB concept of the Liquid Immersion Blanket (LIB) proposed in [32]. The LIB is a self-cooled BB concept based on a molten salt, FLiBe (Li_2BeF_4), which acts as coolant, breeder, and tritium carrier. The name stems from the fact that the vacuum vessel (VV) is submerged in the liquid breeder, which is contained in a large tank. Structural support keeps the vacuum vessel in position. Unlike most conventional concepts, the VV is contained within the blanket, and not the opposite. The configuration investigated as a starting point for this work is broadly consistent with the layout proposed by [33] with the exception that the solid beryllium layer between the two vessel walls has been removed, as formerly proposed by [34]. The structural material considered in all configurations is Inconel 718 and FLiBe flow paths include several channels to actively cool down the FW, divertor channels, VV, and the tank itself. Liquid BB concepts are highly attractive due to their architectural simplicity and low-pressure operation; given that the objective of this paper is to validate the workflow, the intrinsic simplicity of the LIB breeding blanket internals was deemed suitable.

2.1. Parametric neutronic analyses

The objective of the present analysis is to support the preliminary design by performing a sensitivity study on selected geometric and material parameters of the blanket in line with previous studies [35,36]. This step provides quantitative evaluations of key neutronic performance metrics (such as TBR, power density, dpa, neutron fluxes, etc.) and offers insight into the design variables that most strongly influence tritium breeding, neutron leakage, and power deposition. (Fig. 2)

The neutronic analyses presented in this work are performed using the Monte Carlo particle transport code OpenMC [37]. All transport calculations are carried out using the ENDF/B-VIII.0 nuclear data library [38].

For the present pre-feasibility study, the neutronic model is implemented using a simplified Constructive Solid Geometry (CSG) approach, shown in Fig. 3. Due to the perfect toroidal symmetry of the system, the

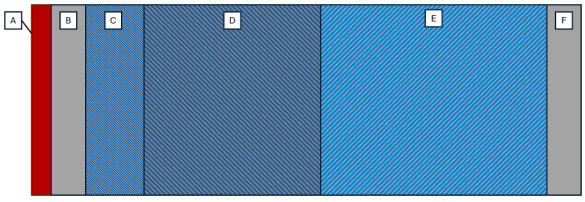

Fig. 2. Schematic cross-sectional representation used for illustrative purposes.

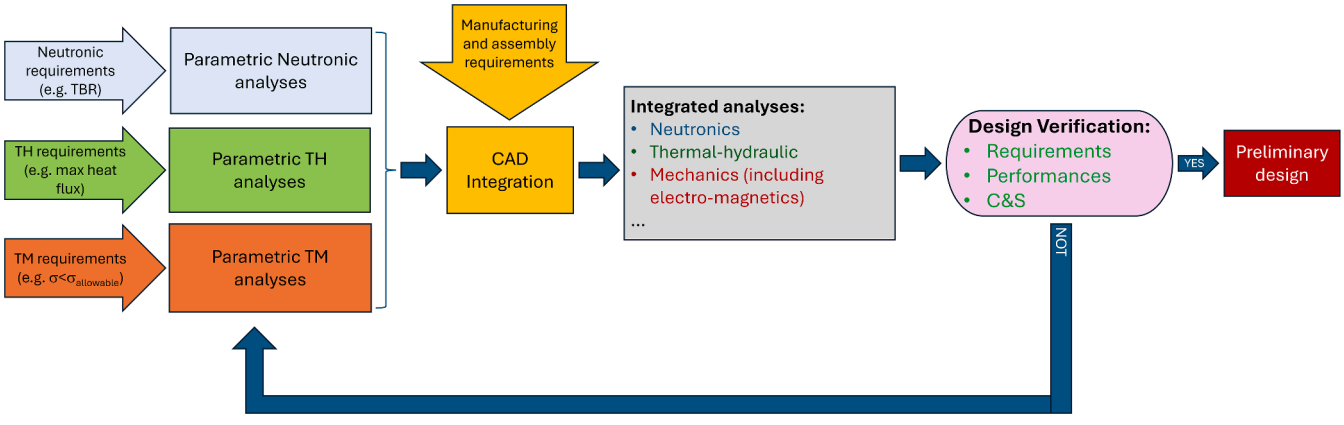

Fig. 1. Simplified workflow employed for BB design.

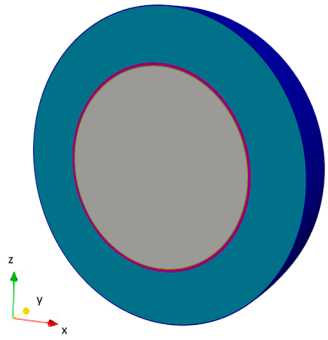

Fig. 3. Toroidal CSG model used for the parametric neutronic analysis.

neutronic analysis was restricted to a 10° sector, allowing a substantial reduction in computational cost without loss of accuracy [39]. This modelling choice is driven by the need to perform an extensive parametric exploration across multiple blanket configurations, material compositions, and radial builds, while maintaining manageable computational costs. At this stage, the objective is not to reproduce the full geometric complexity of a reactor-grade breeding blanket, but rather to identify promising design trends, quantify sensitivities to dominant parameters, and assess compliance with essential physics requirements under simplified yet physically meaningful assumptions.

The total available thickness for the radial build is kept fixed ($\sim$ 1.07 m) and within this constraint both material compositions and thicknesses of selected layers were systematically varied as reported in Table 1. Regarding geometric parameters, the first wall tungsten thickness (zone A) was investigated for three values (1, 3, and 5 mm), while the outer VV thickness (zone D) was varied between 40, 55, and 70 mm. The breeder thickness is reduced from the baseline value as the FW and outer VV thicknesses are increased.

As regards material composition, material volume fractions were also perturbed in multiple blanket regions. In the coolant channels zone (zone C), two FLiBe–structure mixtures were considered (67% FLiBe / 33% structural material and 90% FLiBe / 10% structural material). For the outer VV layer (zone D), FLiBe was introduced at increasing volumetric fractions (10%, 15%, and 20%) to account for a possible second row of coolant channels. A similar approach was applied to the breeder zone (zone E), where the FLiBe fraction was progressively reduced from 90% to 80% and 70%, with the remaining volume occupied by structural material. This was done to account for possible internals (attachment systems, feeding pipes, flow distributors) that, at this early stage, are not considered but may impact neutronic performance (e.g., reduction of the TBR).

Finally, a parametric sweep of the lithium isotopic enrichment was carried out, considering natural lithium and enrichments of 30%, 60%, and 90% in ^{6}Li.

The full parametric sweep resulted in a total of 648 neutronic simulations, each corresponding to a unique combination of layer thicknesses, material fractions, and lithium enrichment.

This dataset enables a systematic identification of the design parameters that most strongly govern tritium breeding, neutron leakage, and power deposition. Moreover, these analyses provide insightful indications to the designers about the average material composition that should be maintained in the different reactor regions to fulfil the requirements linked to neutronic performance.

The resulting database enables a wide range of sensitivity analyses to be performed. For instance, the dataset can be filtered to retain only configurations achieving a TBR $\geq$ 1. This criterion alone significantly reduces the design space, leaving only 25 viable configurations out of the original total cases. In addition, the database provides a reusable framework for future neutronic evaluations, eliminating the need to repeat the entire parametric campaign.

As a first step in exploring the database, a high-level overview of tritium breeding performance is provided.

Fig. 4 reports the maximum TBR value obtained for each combination of first wall (region A) thickness, outer vacuum vessel (region D) thickness, and lithium enrichment level. Each reported value corresponds to the maximum among 18 different configurations, associated with the various combinations of FLiBe volumetric fractions in the cooling channel (region C), in the region D, and in the breeder region (region E).

A comparison among the panels clearly highlights the penalizing effect of increasing the region D thickness on the TBR. When increasing the Outer VV thickness from 40 mm to 55 mm and subsequently to 70 mm, a systematic reduction of the maximum TBR is observed for all combinations of FW thickness and lithium enrichment, emphasizing the dominant role of the Outer VV in attenuating the neutron flux between the source and the breeder.

Similarly, the influence of the FW thickness is found to be significant: none of the configurations characterized by a 1 mm-thick FW achieve TBR values above unity.

For the geometrically most favorable configuration (FW = 5 mm, Outer VV = 40 mm), Fig. 4 shows that TBR values exceeding unity can already be achieved with a lithium enrichment of 30% in ^{6}Li. With a 60% ^{6}Li enrichment, the TBR reaches a value already close to the maximum, which is obtained by further increasing the enrichment to 90%. This additional increase results in only a marginal improvement, of approximately 0.2%. However, a more comprehensive analysis of the database indicates that the configuration with 90% ^{6}Li enrichment is overall preferable compared to the 60% case. In particular, it is characterized by an approximately 5% lower average volumetric power density deposited in the first wall and by a 34.4% reduction in the neutron current escaping from the tank surface.

Fig. 5 presents the TBR values for the subset of configurations characterized by a 5 mm-thick first wall, a 40 mm-thick outer vacuum vessel, and lithium enriched to 90% in ^{6}Li. Fig. 6 provides a more detailed analysis of the neutron current escaping from the tank for this subset of configurations. The analysis shows that the configuration achieving the maximum TBR, corresponding to the case in which the FLiBe volumetric fractions are maximized in all three regions, does not guarantee the best neutron shielding performance. In particular, a reduction of the FLiBe fraction in the breeder region results in an improvement in neutron shielding of approximately 50%.

These results demonstrate that maximizing the TBR alone is not sufficient to identify the optimal configuration. Instead, all the relevant figures of merit must be evaluated jointly, further motivating the adoption of an integrated multiphysics approach, as implemented in the present study.

Table 1
Design parameters included in the neutronic sensitivity analysis, covering geometric and material variations.

Region	Thickness [mm]	Materials		
		Tungsten [%]	Inconel 718 [%]	FLiBe [%]
A	1 – 3 – 5	100		
B	3		100	
C	12		33 - 10	67 - 90
D	40 – 55 – 70		90 – 85 – 80	10 –15 –20
E	1000		10 – 20 – 30	90 – 80 – 70
F	20		100	

2.2. Parametric thermal-hydraulics analyses

The in-vessel components of a tokamak reactor are exposed to extreme conditions, primarily due to intense power deposition from neutron–matter interactions and severe heat fluxes on plasma-facing surfaces.

Therefore, confirming the structural integrity of the BB system

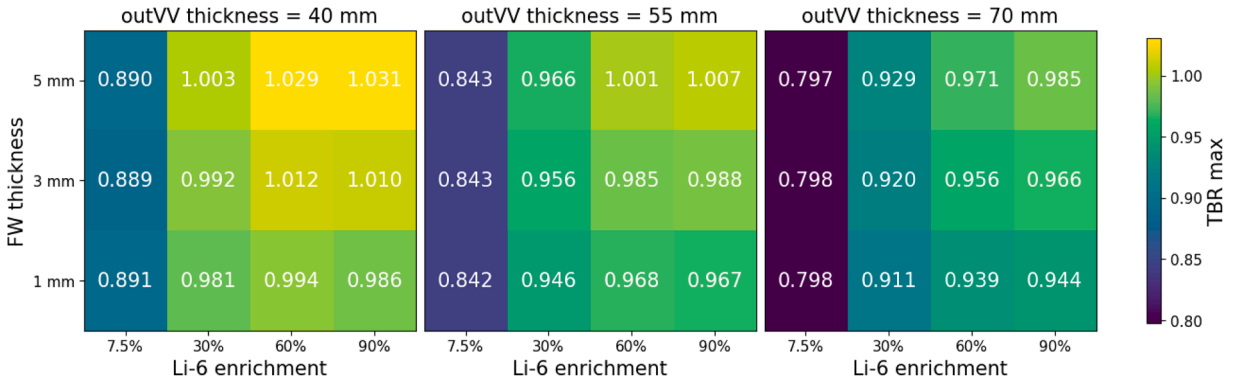

Fig. 4. Change in maximum TBR as a function of first wall thickness and lithium enrichment, for three different outer vacuum vessel configurations.

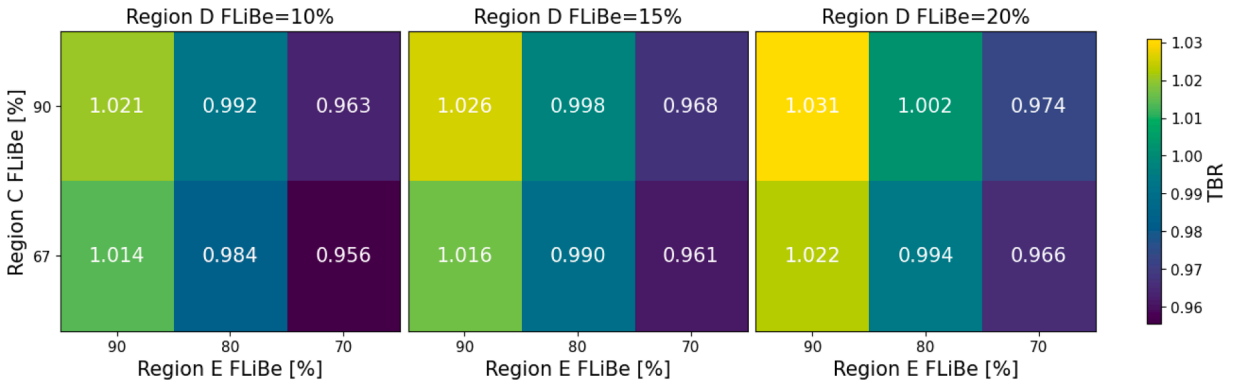

Fig. 5. Change in TBR with FLiBe volumetric fractions in regions C, D, and E for the configuration characterized by FW = 5 mm, Outer VV = 40 mm, and 90% ^{6}Li enrichment.

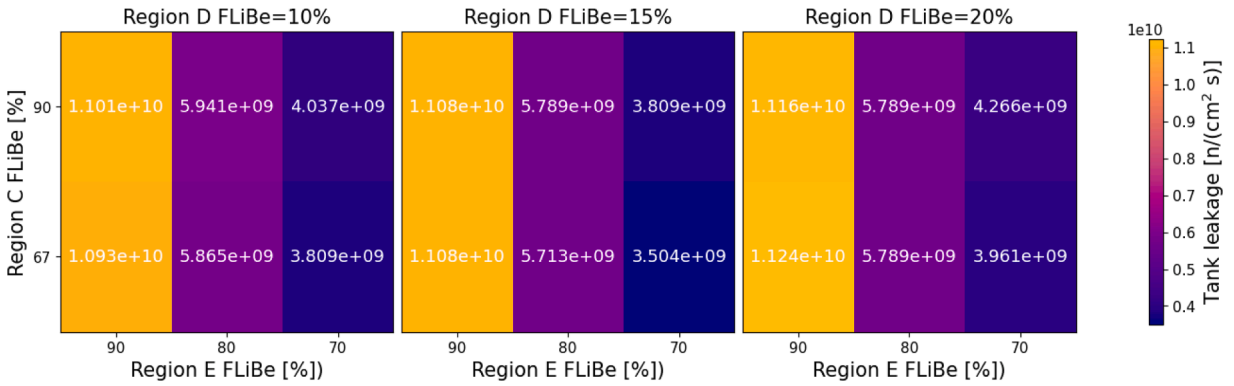

Fig. 6. Change in neutron leakage with FLiBe volumetric fractions in regions C, D, and E for the configuration characterized by FW = 5 mm, Outer VV = 40 mm, and 90% ^{6}Li enrichment.

requires a precise assessment of the flow field and heat transfer. Considering that different heat loads may be encountered depending on the location of the wall-interfacing plasma (i.e., equatorial or divertor areas), various technical solutions should be investigated.

An average heat flux of 0.4 MW/m2 was assumed for the first wall, whereas the divertor region was modeled using a gaussian heat flux profile with the same base level of 0.4 MW/m2 and a peak value of 20 MW/m2, characterized by a standard deviation of few centimeters.

The simulation campaign was structured into several phases:

1. To guarantee accurate numerical results, evaluation of grid independence using various mesh configurations, particularly in the pipe core, was carried out.
2. Passive Heat Transfer Enhancement Techniques (PHETs) free baseline simulations.
3. Assessment of coolant channel geometry, exploring how pipe cross-section, size, and distance from the first wall influence heat transfer.
4. Comparison between different cooling strategies: a. Single pipe: maximum mass flow rate in the divertor but higher inlet temperature for the vacuum vessel. b. Double pipes: reduced flow to the divertor but cooler coolant entering the vacuum vessel. The final choice depends on meeting temperature limits in both components.
5. Simulations with PHET (in case temperatures were above the limits), revisiting prior results [40] and introducing technical solutions, available in literature, such as wire coils, swirling tapes and V-ribs to almost double the heat transfer coefficient compared to plain pipes.

In the case of the divertor area, given the huge differences in terms of heat fluxes with respect to the rest of the first-wall, dedicated design solutions have been identified for the two areas.

The study's initial phase concentrated on simulations using the VV cooling configuration without PHETs (steps 1 through 4). For the model, boundary conditions, material layers, thermophysical characteristics, and volumetric nuclear heating sources were specified. The number of cells across the FLiBe pipe cross-section was the primary difference between the two meshes that were tested. To accurately capture thermal boundary layers, the near-wall resolution ($y+ \approx 1$) was maintained. Grid independence was demonstrated by the perfect matching of the resulting temperature profiles. Increasing the distance *d* between the coolant pipe and the FW, altering the cross section (circular, rectangular, or square), raising the channel height *z*, and examining the impact of single versus double channels on the FW temperatures were all done using parametric analyses. (see Fig. 7).

According to preliminary analyses, the system's thermal behaviour is greatly impacted by changes in the distance d between the coolant channel and the FW. As d increases, the temperature of the FW rises by about 50 K while the temperature of the tank side wall decreases by about 20 K.

These patterns were validated by additional studies that compared various coolant channel geometries. While a square or rectangular channel offers more flexibility for thermal control, a circular pipe raises FW temperatures and lowers tank side temperatures. The temperature distribution can be adjusted by changing the section height (*z* dimension). As *z* increases, the tank side temperature decreases, but the FW temperature rises due to the lower coolant velocity that comes with a larger cross-sectional area.

Finally, effect of single-channel versus double-channel configurations is assessed. In the first configuration the whole coolant flow rate enters the divertor and, after exiting and heated up, it cools down the VV. In the double-channel configuration, the flow rate is split, and a fraction goes directly to the VV. However, results show that the thermal advantage of the double-channel approach is limited. Indeed, the divertor cooling is disadvantaged as the inlet temperature remains the same but the mass flow rate is reduced; on the other side, the reduction in FW temperature is negligible, although the tank-side temperature improves (i.e. reduces) by approximately 20 K (see Fig. 8).

The PHET-equipped exploration technologies were driven by the requirement to keep solid structures below critical temperature limits. For the sake of conciseness, we concentrate hereon on V-shaped ribs, which were chosen for their robust performance at low Reynolds numbers that are compatible with a generic FPP operating conditions. By creating secondary flow structures, increasing surface turbulence, and periodically disrupting the flow, V ribs improve heat transfer. V ribs produce two separate vortical structures, offering better mixing than straight ribs, which produce a single recirculation cell. Several geometric parameters influence their behaviour: pitch, attack angle (θ), rib shape, presence of gaps (discrete ribs), layout, and distribution across channel walls.

A double-channel VV geometry with 120° V ribs, 10 mm pitch, and 1 mm rib height, positioned on the upper and lower walls, was the subject of an initial analysis. When compared to a plain channel, the ribs greatly lowered wall temperatures by increasing turbulence and encouraging strong secondary flows. There were temperature drops of roughly 40 K at the tank wall and 90 K at the first wall. Furthermore, parametric studies of the V-ribs pitch (10 mm and 20 mm) or attack angle (120° and 90°) were also investigated.

In the divertor area, significantly higher heat fluxes are anticipated (>10 MW/m^2), making cooling more difficult. Two designs (Configurations A and B) were assessed for varying thicknesses of Inconel and tungsten. The data presented in Fig. 9 were used for parametric analyses.

In this investigation, configuration A consistently outperformed configuration B. Moreover, it was found that the limiting constraint was the temperature in the structural material. Indeed, as can be seen below, the critical temperature was reached first in the Inconel region near the FW, not in the tungsten.

Additional cooling enhancement strategies were investigated, such as the Jet Impingement Cooling (see Fig. 10).

The studies have shown that the division of the jet created a central recirculation zone, reducing local heat transfer. As a result, FW temperatures were higher than in the ribbed-channel case, making this configuration less advantageous. For this reason, this solution was discharged.

Lastly, also magnetohydrodynamic (MHD) effects were considered, assuming a toroidal magnetic field equal to 10 T and assessing the Lorentz forces on the coolant and Joule heating. Because RANS models do not inherently account for turbulence suppression due to magnetic damping, a modified Reynolds Stress Model incorporating an additional sink term was implemented. Results showed that pressure drop increases dramatically: 3 × in plain channels, 1.5 × with V-ribs while heat transfer

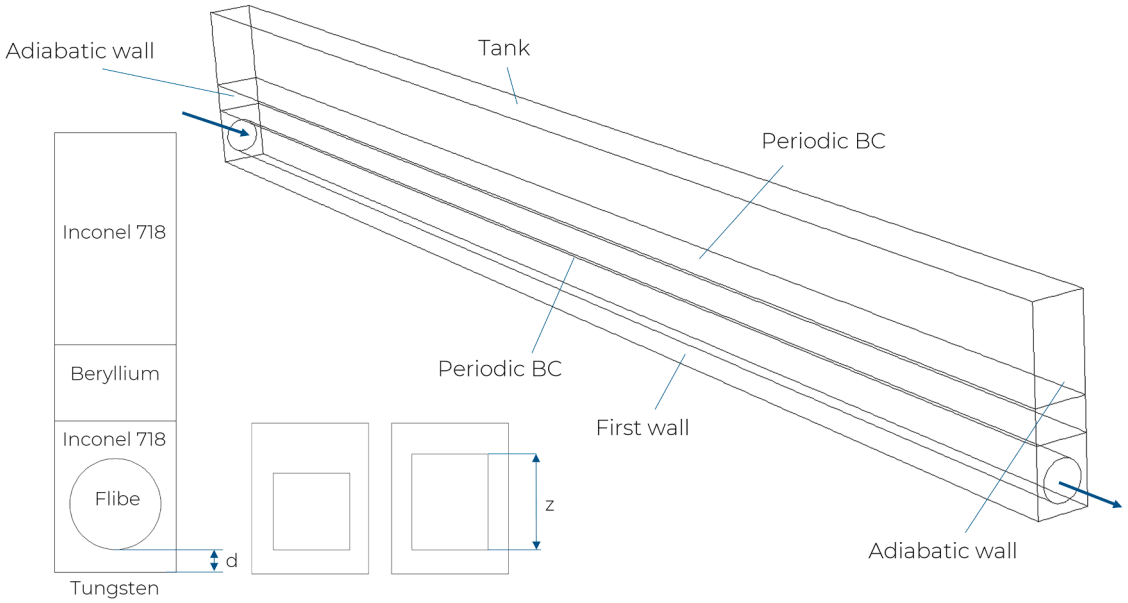

Fig. 7. Geometrical configuration and materials for the VV.

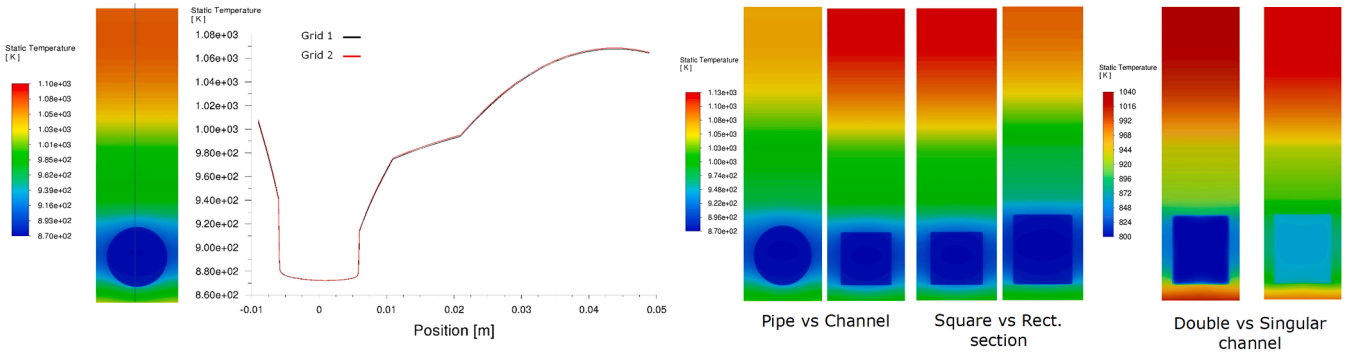

Fig. 8. Examples of FW thermal-hydraulic parametric results.

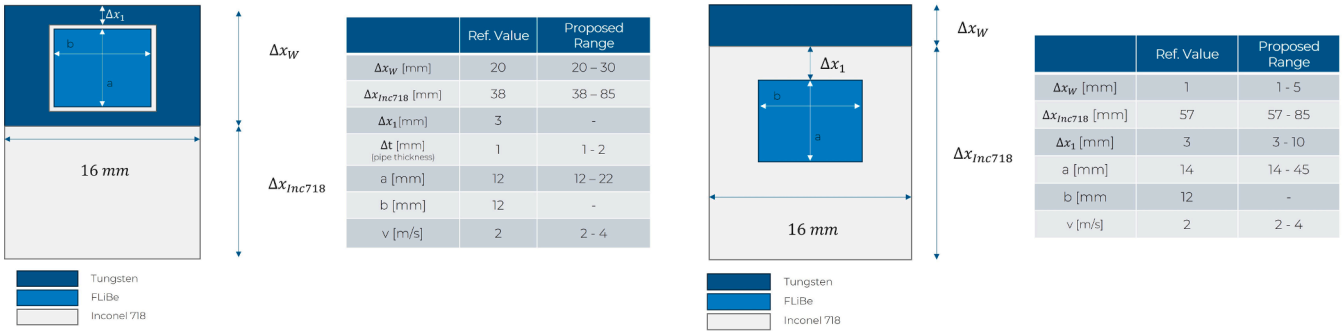

	Ref. Value	Proposed Range
Δx_W [mm]	20	20 – 30
Δx_{Inc718} [mm]	38	38 – 85
Δx_1 [mm]	3	-
Δt [mm] (pipe thickness)	1	1 - 2
a [mm]	12	12 – 22
b [mm]	12	-
v [m/s]	2	2 - 4

	Ref. Value	Proposed Range
Δx_W [mm]	1	1 - 5
Δx_{Inc718} [mm]	57	57 - 85
Δx_1 [mm]	3	3 - 10
a [mm]	14	14 - 45
b [mm	12	-
v [m/s]	2	2 - 4

Fig. 9. Configuration A and B, respectively, for the divertor and its range of variability.

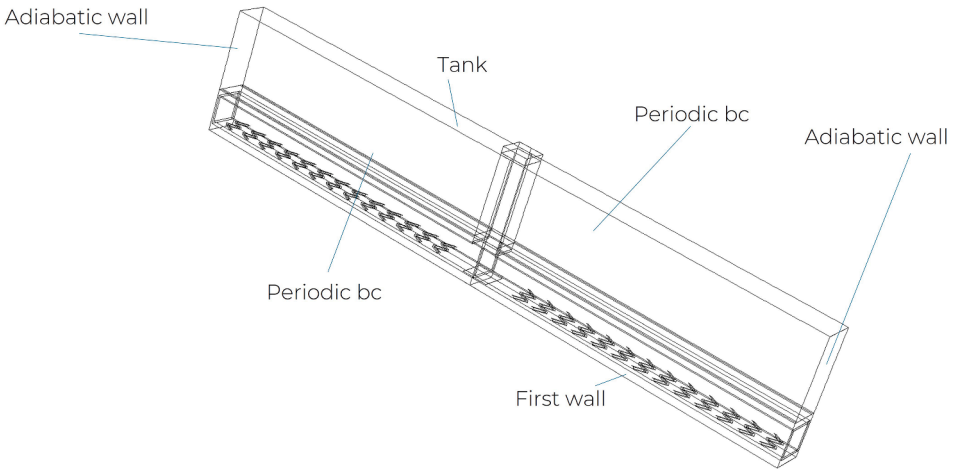

Fig. 10. Jet impingement configuration.

coefficient reduction is surprisingly small (~1.3% loss in plain channel and nearly negligible with V-ribs). These results suggest that PHET-induced turbulence compensates for MHD laminarisation, although additional validation is required to confirm the accuracy of the energy equation treatment.

After all these considerations, it was clear that, for the given conditions, the V-ribs configuration was the most promising. Therefore, a parametric analysis was performed to identify maximum acceptable heat loads when limiting temperatures to $T_{Tungsten} < 1500\ K$, $T_{Inconel718} < 1050\ K$ and a more conservative limit of $T_{Inconel718} < 923\ K$.

By means of these parametric analyses, it was possible to determine the maximum heat flux tolerated by the divertor first wall to maintain the materials temperature below the critical value. As can be observed, the limiting material is the Inconel718, reducing by a factor of 3 (or about 7 in the worst case) the allowable heat flux depending on the different velocities (see Table 2).

Table 2
Maximum heat flux depending on the material temperature limit and FLiBe velocity.

	FliBe velocity = 4 m/s Max heat flux [MW/m2]	FliBe velocity = 6 m/s Max heat flux [MW/m2]
Tungsten Temperature < 1500 K	7.5	10.5
Inconel 718 Temperature < 1050 K	2.5	3.5
Inconel 718 Temperature < 923 K	1.1	1.6

2.3. Parametric thermo-mechanical analyses

Due to the extreme heat loads on BB, significant temperature rises occur during operation, leading to non-negligible thermal expansion. This effect must be carefully evaluated through dedicated thermo-mechanical (TM) simulations to determine the resulting displacement fields and associated stress states, which are critical for structural integrity assessment.

Therefore, at the outset of designing any BB concept, it is essential to perform targeted and parametric TM analyses to optimise the geometrical configuration of the proposed design, to be compliant with both thermal management and structural integrity.

At this stage of the design process, simplified analyses are considered to investigate preliminary solutions and to perform the first round of optimisation. The inboard section of the FW and VV is identified as the most critical area for investigation because of high neutron wall loads and heat fluxes expected. To this end, a 2D parametric finite element (FE) thermal model, solving the steady state heat diffusion equation, of an inboard poloidal cross-section has been developed using ANSYS APDL [41]. The location of the cross-section is highlighted in Fig. 11. As illustrated, the cut is positioned slightly above the equatorial plane, where cooling channels remain perfectly orthogonal to the section, rather than at the equator, where the ducts begin to deviate toward the FLiBe tank. This choice ensures that the section is representative of the average FW design. Furthermore, the toroidal symmetry of the hydraulic circuits has been exploited to reduce the computational domain to a 5° sector, given that the proposed hydraulic circuit exhibits a 10° toroidal periodicity.

Together with the position of the cut, in Fig. 11, the reference cross-section configuration is shown as well, together with the drivers (plasma heat flux and volumetric heat generation due to neutron-matter interactions) as well as the considered boundary conditions, namely the Robin boundary conditions imposed within the cooling channels and on the tank side and the contact thermal conductance between the Beryllium, which serves as neutron multiplier, and the structural material (Inconel 718). For all the Robin boundary conditions, the reference temperature is estimated to be equal to the inlet FLiBe temperature plus 60% of the foreseen ΔT. In the case at hand, as suggested in [34], the FLiBe inlet temperature is considered equal to 773 K and the overall ΔT equal to 60 K, thus obtaining a reference temperature of approximately 810 K.

The parametric thermal model has then been adopted to investigate several different options in terms of cooling channel arrangement and geometry, ensuring that the temperature remains below 650 °C (923 K) within the structural material (the critical temperature for creep) and below the recrystallisation temperature for tungsten.

An overview of the geometrical parameters as well as the capabilities of the parametric model is shown in Fig. 11 on the right. The design approach followed in this work allowed the investigation of different parameter effects and the identification of an optimal solution in terms of temperature and stress field. In particular, the following parameters were investigated:

1. changes in the number, shape (i.e. round or rectangular) and position (i.e. pinch, distance from the wall, etc.) of the channels,
2. to have or not a second row cooling the outer VV,
3. to include or not the Beryllium neutron multiplier and in which form,
4. changes in the inlet and outlet temperature of FLiBe,
5. changes in the FLiBe mass flow rates,
6. changes in the structural material (Inconel 718 or Hastelloy N)

At the end of the optimisation, a configuration respecting the material temperature limits almost everywhere has been identified, characterised by two parallel rows of square cooling channels, without any intermediate layer of neutron multiplier. The temperature map for the structural material in the optimised case is reported in Fig. 12, capping the legend at 650 °C (923 K) so that the regions not respecting the creep limit are highlighted in grey. As is possible to observe, the temperature is, on average, well below the limit. A single hotspot is observed at the plasma side in the connection region between neighbouring segments, where larger spacing is present due to the presence of the welding bevel (top right corner in Fig. 12). The temperature field is, however, considered satisfactory and used as a driver for the thermo-mechanical analysis.

Before going to the thermo-mechanical analysis, a preliminary check on the primary stresses has been performed by applying the foreseen pressure loads, showing no issues in terms of structural integrity.

To obtain more realistic results in terms of stress state, the thermo-mechanical simulation has been performed on a straight 3D segment of the inboard region with symmetry conditions on the sides and on the bottom of the segment and imposing plane strain behaviour on top of it, to preliminarily mimic the overall segment behaviour.

Applying the obtained temperature field and the design pressure load within the channels and on the tank side, the equivalent Von Mises stress field, shown in Fig. 13, is obtained.

The obtained stress field has been used as input to the structural integrity assessment procedure following the design rules prescribed by the ITER SDC-IC along seven different critical paths for stress linearization. For all the paths satisfactory safety margin (~ 40% or above) has been obtained, both considering low and high temperature rules.

The results obtained from this preliminary structural integrity assessment allow for the integration of the proposed configuration within a detailed CAD, which would become the starting point for the following integrated analyses.

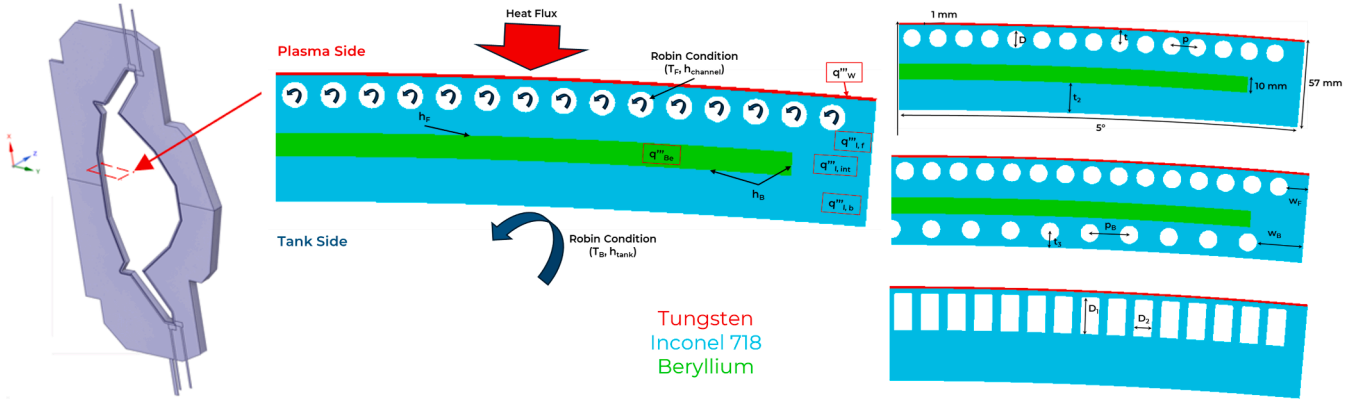

Fig. 11. 5° BB segment with highlighted the position of the cross-section considered for the 2D FE thermal model. Representation of the reference cross-section to be optimised is included as well (mostly taken from [33] and [40]).

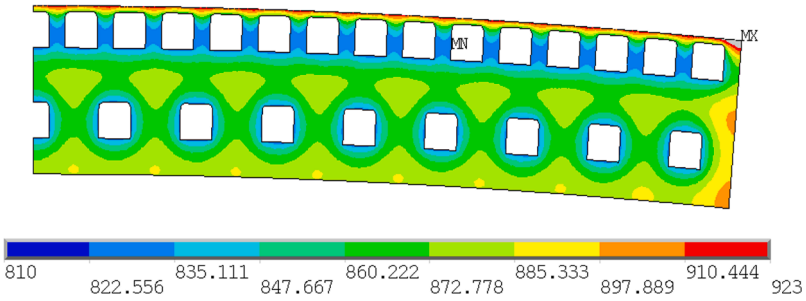

Fig. 12. Inconel 718 temperature field capped at creep temperature limit (923 K) in the optimised case.

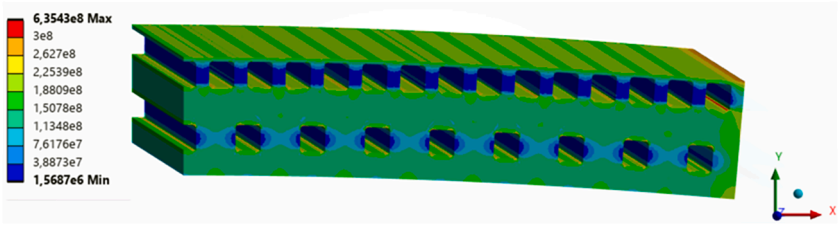

Fig. 13. Equivalent Von Mises stress on mid-section plane considering thermal expansion and pressure loads. Results expressed in Pa.

2.4. From the CAD integration to the final design

This section describes a staged workflow that builds on the findings of the blanket design-space exploration (i.e. parametric studies). It (i) condenses parametric results into workable design patterns, (ii) synthesizes them into a single, manufacturable integrated CAD, (iii) performs neutronic, thermal-hydraulic, and thermo-mechanical analyses on that common geometry, and (iv) iterates effectively when requirements are not met by either extending the design space when necessary or reusing previously explored parametric solutions. This method expedites convergence to a compliant design, breaks down complexity early, and maintains requirement traceability throughout.

2.4.1. From parametric analyses to candidate solutions integrated in CAD

In this step, the variety of parametric explorations is transformed into a carefully selected set of design solutions, each validated for single physics performance and compliance with the relevant requirement subset. These solutions are then combined into a cohesive geometric concept that is prepared for integration. In fact, the parametric sweeps over important geometric/process variables (such as first wall thickness, channel pitch/shape, rib spacing, manifold cross sections, gaps/clearances, divertor tile geometry) and the single physics acceptance criteria and margins (such as nuclear heating distribution bounds, maximum FW surface temperature, minimum pressure drop/flow distribution uniformity, stress/strain/fatigue limits) are screened and shortlisted from the parametric database, along with their sensitivity and robustness indicators.

2.4.2. Integrated CAD synthesis with manufacturability, Weldability, and "Assemblability"

In this step, a reference CAD model is created. It combines the chosen design features while addressing Design for Manufacturability (DfM), Design for Weldability (DfW), and Design for Assembly (DfA). This approach ensures that geometric accuracy, process feasibility, and downstream integration are tackled together, rather than being fixed later on. It is important, at this stage, to contact technology vendors and to integrate their indications. Indeed, particular attention should be given to the following aspects based on guidance from technology vendors and manufacturers:

- **Manufacturability**: parameters such as minimum wall and rib thicknesses, achievable bend radii, casting and machining allowances, tolerance stacks, distortion allowances, surface finish requirements in high heat flux zones are considered. Access for tooling and non-destructive evaluation should be considered as well.
- **Weldability**: aspects related to (i) the joint preparation standards, such as corners and full penetration, (ii) weld sequencing to reduce residual stresses, (iii) compatibility with proposed processes, including TIG, EBW, HIP, and brazing, (iv) inspection volumes and coupon locations and (v) heat affected zone margins next to coolant channels should be considered.
- **"Assemblability"**: it should be considered the poloidal and toroidal segmentation strategy, schemes and alignment features, interface envelopes to the VV, divertor (and ports), integrated lifting and attachments points, maintainability and replacement paths.

As an example, for the FPP BB concept herewith used as case study, the FW and divertor configurations optimised through the parametric campaign are inserted into the CAD. The layout of coolant channels, transition zones, and manifolds is preliminarily routed, and initial poloidal segmentation and weld joints are defined to support structural integrity and seamless hydraulic integration. Fig. 14 illustrates the integrated model.

2.4.3. Consistent integrated multi-physics analyses on the integrated CAD

At this point, using the same integrated geometry and synchronised material/operational assumptions, neutronic, thermal-hydraulic, and thermo-mechanical simulations are carried out such that all models are mutually consistent and results are coherent. Indeed, this approach allows for consistency enablers such as:

- **Geometry fidelity (i.e. CAD centric):** the CAD becomes the true source for all the next steps.
- **Field mapping:** the output of one analysis is used as an input for the next ones (e.g. nuclear power density or helium/Tritium production rates calculated via neutronic calculations are mapped into the CFD/FEA meshes, temperature fields and pressure loads calculated via thermal-hydraulic analyses are mapped into the thermos-mechanical model, etc.)

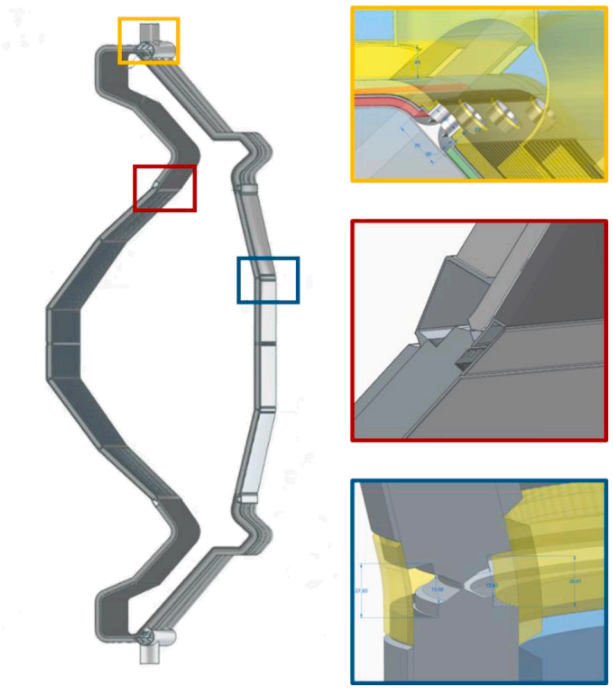

Fig. 14. Integrated CAD model of the vacuum vessel.

At the end of this step, an update of (i) nuclear performance (e.g., TBR, dose/activation, etc.), hot-spot temperatures and Δp, flow distribution, stress/strain/fatigue factors and displacement as well as (ii) a compliance matrix against the requirement set (with margin and uncertainty assessments) is obtained.

2.4.4. Iteration loop: from integrated analyses back to parametric space (and expansion if needed)

It is important to highlight that the design process described above might be affected by non-compliance or insufficient margins during the execution of the integrated analyses. In this case (i.e. when a non-conformity is found), from the integrated analyses, the design process loops back in a controlled manner. Indeed, two pathways might be identified: (i) the solution to the non-conformity has already been investigated in the parametric scan or (ii) new configurations must be explored.

1. **Solution already investigated.** In this case, the previous parametric analyses are used to extract the new feasible solution that is then re-instantiated in the CAD to re-run the integrated analyses.
2. **Solution not yet investigated.** The existing parametric database is enlarged, introducing new parameters or widening bounds (e.g. alternate manifold topology, different segmentation/weld joint types, revised material thickness, modified divertor tile pattern, etc.). Once the solution is found, it is integrated into the CAD and the integrated analysis cycle is repeated.

Of course, this design process must also be supported by system engineering approaches to maintain traceability of the modifications and decisions.

The iteration occurs until all requirements are met with agreed margins under the defined load cases, at which point the CAD is baselined and released for downstream detailing, procurement planning, and qualification test article definition.

2.5. Benefits of the approach

The previous paragraphs have substantiated the design process approach that has been developed for the design of BB systems. This approach, together with Systems Engineering, design codes, and industrial manufacturing standards, is pivotal to the industrialisation of the BB system. Three essential characteristics contribute to this workflow's effectiveness.

- **Structured decomposition and parallelism**. First, a complex problem is decomposed into simpler ones, and parallel developments are possible, performing single-physics parametric studies, which also creates a reusable database of validated design patterns enhanced with robustness and sensitivity data.
- **Requirements embedded end-to-end**. Second, the risk of late-stage non-compliance is decreased because requirements are embedded end-to-end and enforced both during parametric screening and again during CAD integration.
- **Fast, informed iteration with knowledge reuse**. Third, iteration is quick and well-informed. The design space expansion is focused and data-driven. Known solutions can be quickly repurposed. Every iteration improves the body of knowledge, speeds up convergence, and reduces rework, all of which contribute to the timely delivery of a manufacturable and compliant design.

3. Application to tritium fuel cycle

DT fusion reactors are expected to operate with a Tritium Burning Efficiency (TBE), defined as the fraction of tritium burned inside the VV relative to the amount injected, typically ranging between 0.1% and a few percent. This inherently low burn-up rate necessitates the implementation of a closed tritium FC (see Fig. 15) capable of ensuring continuous recovery, purification, and re-injection of tritium into the plasma.

In the architecture here considered, the FC is organized into three process loops:

- The primary closed loop handles the dominant tritium throughput from the plasma exhaust. The Vacuum Pumping System (VPS) routes the exhaust (H/D/T plus helium ash and volatile impurities) to the fuel cleanup train consisting of a Tokamak Exhaust Purification (TEP), Isotope Separation System (ISS) and Storage and Delivery System (SDS) before reinjecting a conditioned D–T mixture to the Fueling Injection System (FIS).
- A derived detritiation loop branches from this primary loop and from ancillary systems (e.g., vacuum forelines, gloveboxes, process equipment enclosures). Its purpose is to treat low-concentration tritium streams in the Atmospheric Detritiation System (ADS), which is followed by a Water Detritiation System (WDS). Since no water is assumed to be used for cooling the in-vessel components of an FPP equipped with a LIB, the WDS is responsible solely for detritiating the tritiated water generated in the ADS. Only after meeting regulatory discharge limits, the effluents are routed to the plant stack or liquid waste handling, ensuring defence-in-depth for environmental protection. This loop operates at comparatively low tritium throughputs but is critical for bounding normal and off-normal emissions.
- The Outer Fuel Cycle loop manages tritium generated in the BB. According to the BB design presented in Section 2, FLiBe is continuously circulated through the BB to exhaust the fusion power. As it exits the BB, FLiBe flows through the Tritium Extraction System (TES), where a fraction of tritium is removed from it. Lastly, FLiBe flows through the Heat Exchanger (HX) and is delivered back to the blanket. Therefore, the primary heat exchangers are part of this loop for FPP employing a LIB. Because FLiBe performs both functions, the systems responsible for heat removal and fuel breeding are closely linked. As a result, terms like Primary Heat Transfer System and Outer Fuel Cycle are often used interchangeably.

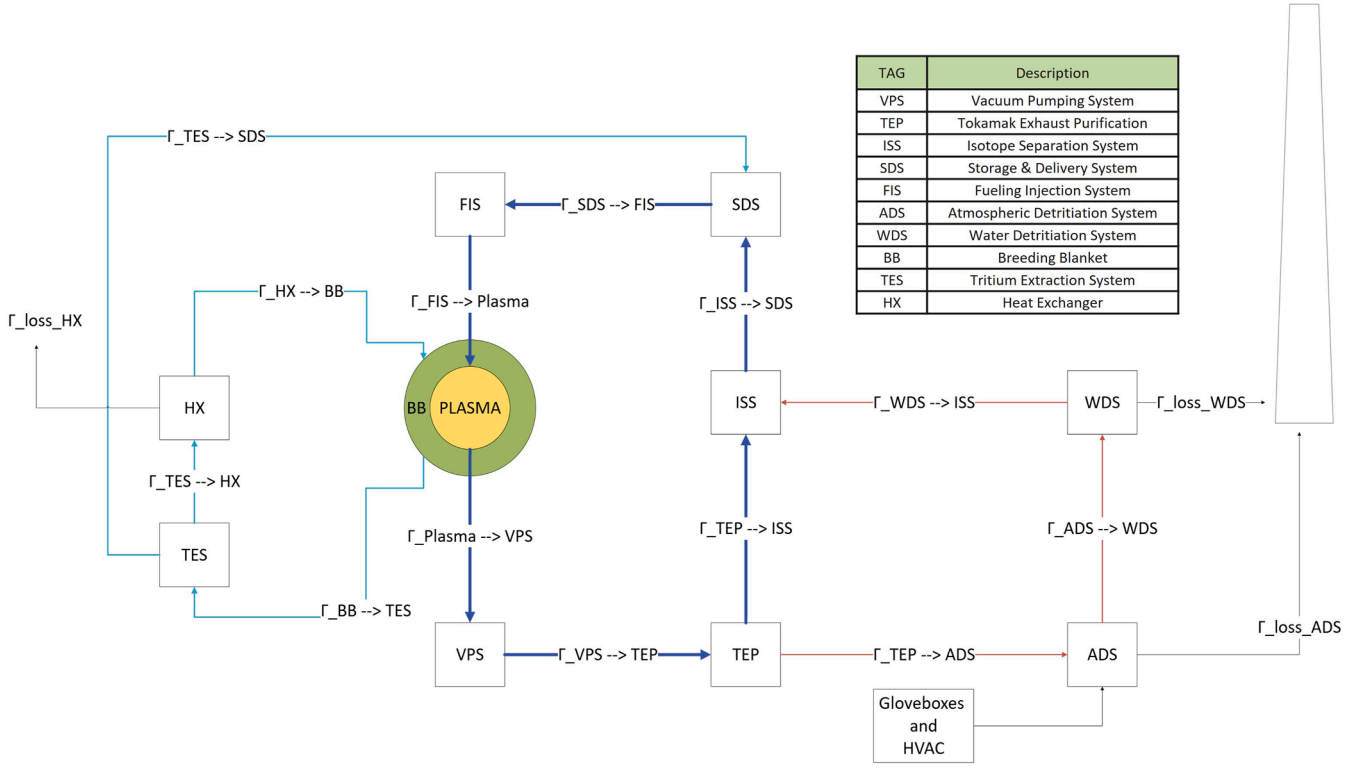

Fig. 15. Schematic representation of the inner and outer fuel cycle.

Once the FC architecture has been selected, a sub-system level design stage has been developed following a standardized workflow for which a simplified flow diagram is shown in Fig. 16 [31].

The design approach for each fuel-cycle subsystem begins with the definition of the basis of design and the identification of high-level requirements, which guide the assessment of the available technological options. In the subsequent phase, process simulations and component-sizing studies are performed to explore the design space and to understand the behaviour of the sub-system under different operating conditions. The outcomes of these analyses are progressively consolidated into a process flow diagram (PFD) and associated product specifications. These results are then integrated into a comprehensive Equipment List including, for each equipment identified in the PFD, dimensions, power needs, relevant duties and operating conditions. Here, specifically for fuel cycle sub-systems, the equipment list is complemented with an estimation of the tritium inventory for which dedicated guideline has been developed to establish a consistent, transparent, and traceable framework for estimating tritium inventories across all FC units. The outcome of this analysis is then verified against requirements, i.e. expected performance, and compliance and safety aspects. This iterative workflow enables the early identification of weaknesses or inconsistencies, ensuring that design improvements can be introduced before moving to the next stage.

This subsystem-level workflow is embedded within a broader system-level workflow (Fig. 17). At the system level, the need is to coordinate and integrate the outputs of all fuel-cycle subsystems to ensure coherence with the overall plant architecture. Starting from the Basis of Design and high-level requirements, a reference FC architecture is selected, defining subsystem boundaries, functional interactions, and major process interfaces. Each subsystem is then developed in parallel following the aforementioned standardized workflow. Their results are then consolidated within a system-level analysis phase, where the whole design is evaluated to verify global consistency and identify cross-subsystem dependencies or conflicts that may not be visible at the

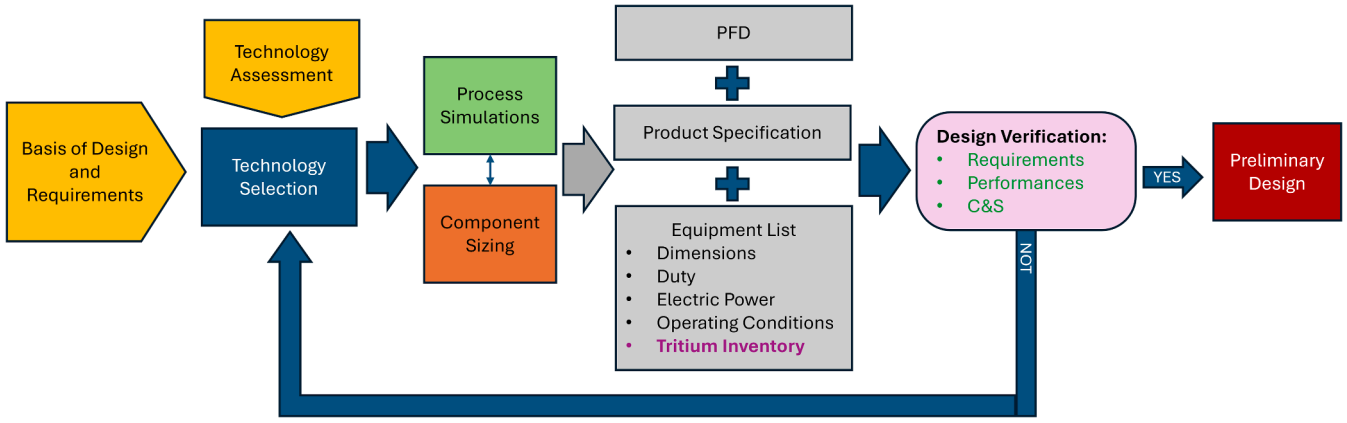

Fig. 16. Simplified flow diagram employed for sub-systems in the FC design.

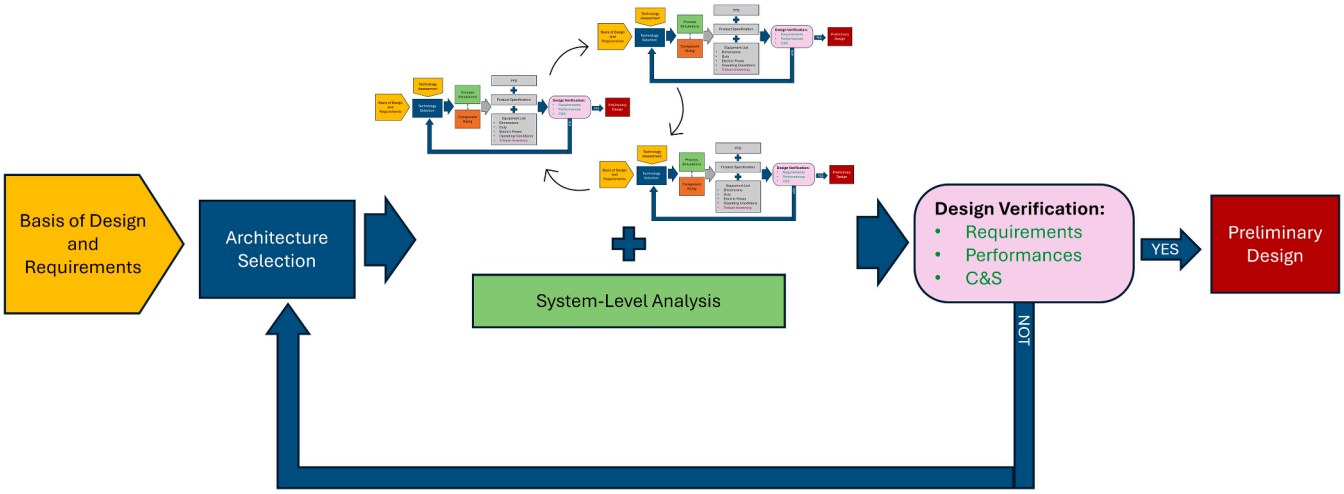

Fig. 17. Simplified flow diagram employed for the FC design.

subsystem scale. The integrated FC configuration is subsequently assessed against functional, performance, and compliance and safety requirements. If the design does not meet these criteria, the workflow triggers iterative feedback loops that may involve the revising of architectural choices.

Given the current stage of FPP development, reactor input data and system requirements remain highly uncertain and are far from finalisation. To enable progress in the preliminary design according to the adopted workflow, an initial set of assumptions was established. These assumptions cover key parameters such as fusion power, TBE, plasma exhaust composition, and release limit constraints. These parameters serve as main inputs for subsequent modelling, simulation, and design analysis processes. Operational requirements and target efficiencies are established based on literature data, industry standards and best practices. Each assumption has been systematically documented to ensure transparency, traceability, and adaptability as more accurate data become available. This structured approach provides a flexible foundation for iterative refinement and sensitivity analyses as the design matures. In the following, an example of the workflow procedure applied to ISS sub-system is reported.

3.1. Basis of design for the ISS

The development of the Basis of Design (BoD), including sub-system boundary conditions and requirements, requires both a higher-level design stage, from which subsystem-level requirements are propagated, according to the V-model approach, and a rigorous interface management at sub-system level. To ensure consistency, traceability, and compliance with design standards, a dedicated document specifying the BoD for each sub-system is maintained throughout the development process. A proper definition of the BoD at this initial stage is essential to enable well-structured systems engineering activities, including requirements management and interface control.

Examples of interfaces managed by the ISS include the feed streams originating from the TEP, responsible for removing helium ash and PEGs from the plasma exhaust, and from the WDS. The TEP-derived feed mainly depends on fusion power, TBE, and TEP efficiency. In contrast, the WDS-derived feed is influenced by the limited information currently available on the air streams entering the ADS, together with the performance of the wet scrubber and the specific design assumptions adopted for the WDS. Because these latter parameters rely on secondary assumptions and remain poorly constrained in this first design iteration, the resulting Q2 stream from the WDS is subject to considerable uncertainty. Representative examples of feed streams from the TEP and WDS to the ISS are reported in Table 3.

Table 3
Example of feed streams to ISS.

Line	Q2 from TEP	Q2 from WDS
Mass Flow Rate (g/h)	539.3	2310.0
Tritium Mass Flow Rate (g/h)	316.5	2.1E-3

With respect to ISS requirements, an excerpt of the requirement table is provided in Table 4. The table includes a final column, *Compliance*, which will be completed during the Verification and Validation (V&V) phase in accordance with the adopted V-model methodology.

3.2. Technology assessment and selection

A literature review of the proposed technologies is performed to develop an in-depth understanding of their current state. The goal is to identify existing centers of excellence, assess supply chain maturity, determine the TRL, and highlight gaps requiring further investigation. The subsequent selection process is guided by figure of merits, which may include TRL, energy consumption, physical dimensions, safety, reliability, and tritium inventory.

As regards the ISS, a TRL assessment has been conducted on the technological options according to authors knowledge. The chosen technology for isotope separation is Cryogenic Distillation (CD), which offers the highest separation efficiency for hydrogen isotopes at large scale and was assessed as the technology with the highest TRL for the required operating conditions. Indeed, CD has already been adopted in the past at the Tritium Systems Test Assembly (TSTA) [43] experiments , at the Joint European Torus (JET) [44] and Tokamak Fusion Test Reactor (TFTR) [45] reactors, and in the TRENTA facility at the Tritium Laboratory Karlsruhe (TLK) which is a prototype of the ITER WDS and ISS protium separation column [46]. There are applications also in the fission sector when coupled to a Liquid Phase Catalytic Exchange (LPCE) or a Vapour Phase Catalytic Exchange (VPCE) in a Tritium Removal

Table 4
Example of sub-system requirements for the ISS.

ID_number	Requirement	Reference	Compliance
REQ_ISS_01	The ISS shall separate incoming hydrogen stream into T2, D2 streams.		Y/N
REQ_ISS_02	The ISS shall remove H2 from the torus hydrogen exhaust.		Y/N
REQ_ISS_03	Protium concentration at the outlet shall be below 1%.	[42]	Y/N

Facility for CANDU reactors.

Alternative fuel cycle proposed for other FPP concepts (e.g. STEP [47]), suggest sending the main permeate feed from the TEP directly to the SDS, while only partially separating the deuterium and tritium isotopes in the ISS for fuel rebalancing. Under these conditions, the reduced flow rate would also make it feasible to consider technologies such as Thermal Cycling Absorption Process (TCAP), Membrane Coupled - Temperature Swing Absorption (MC-TSA), or pressure swing adsorption (PSA) as alternatives to cryogenic distillation [48].

3.3. Process simulations and component sizing

To ensure accurate design and performance assessment of the FC, extensive process simulations were carried out. Given its similarities to a chemical process plant, the sub-systems were modeled using Aspen HYSYS® [49], a widely adopted process simulation tool in the Oil & Gas industry. Custom extensions were developed to account for non-standard equipment (such as vacuum pumps) and unconventional fluids (including gaseous tritium and FLiBe), enabling realistic representation of system behaviour. In particular, the four hydrogen molecules (HT, HD, DT, T_2) and the five oxidized isotopologues of hydrogen (HDO, HTO, D_2O, DTO, T_2O), were implemented as pseudo-components in HYSYS®. Their physical properties were thus manually inserted using data from [50]. Furthermore, due to the very low operating temperatures of the columns, all six hydrogen isotopes are present in both vapor and liquid phase in the simulation. Therefore, to ensure accurate vapor-liquid (V-L) equilibria calculations, it was necessary to specify the vapor pressure equation coefficients for all six isotopes within the HYSYS® 'Properties' tool.

The ISS unit was simulated using a cascade of three cryogenic distillation columns. Among the three cryogenic distillation columns, the tritium extraction column operates at the highest cryogenic temperatures (between 24.85 K and 26.15 K). Its feed consists of a hydrogen mixture (Q_2) coming from the TEP unit. After passing through a series of cooling exchangers, the feed enters the column as liquid phase at an intermediate stage of the column.

From the tritium extraction column, two streams are extracted: a tritium-rich stream (>90% T_2) from the bottom of the column and a D–T mixture stream (≈50–50 mol%), which are then both sent to SDS. From the deuterium extraction column, a deuterium-rich stream (>95% D_2) is extracted and sent to the SDS. Before reaching the SDS, all three product streams are reheated to ambient temperature. The second ISS feed originates from the WDS and enters the protium extraction column. From this column, a protium-rich stream is extracted and can be directed either to the WDS or to the stack (or other uses). Each column consists of three components:

- a condenser at the top, which produces a liquid hydrogen flow by cooling the hydrogen gas using helium coolant at 20 K;
- a reboiler at the bottom which generates a hydrogen vapor flow from the liquid hydrogen in the reboiler with an electric heater.
- a packed section in the middle, where vapor and liquid flow countercurrently contacting with each other in the packed section. Packing materials (such as Dixon Ring) exist to get a large surface area and to disperse the liquid flow. An isotope having lower boiling point tends to move to the vapor flow and is finally enriched into the condenser.

The cryogenic distillation columns have been simulated with a Height Equivalent Theoretical Plate (HETP) of 55 mm [51]. Each cryogenic distillation column has been designed considering an appropriate number of theoretical stages, including one additional stage for the condenser and one stage for the reboiler. The corresponding number of structured beds was therefore specified for each column. Interspace between adjacent structured beds were considered to accommodate liquid distributors as well as inlet and outlet nozzles. The contribution of tritium radioactive decay heat was neglected in the present analysis [48].

Equilibrators are also included in the design. These components are catalytic reactors that promote isotope exchange reactions, dissociating hetero-isotopic molecules (HD, DT, HT) and favoring the formation of homo-isotopic molecules (H_2, D_2, T_2), thereby enhancing overall separation efficiency. Operating at room temperature, they help convert these molecules into more easily separable forms before recycling the product back to the column.

All equilibrator reactors were assumed to employ Pt- or Pd-based catalysts. Due to the lack of specific literature data on space velocity for hydrogen isotope equilibrators, it was assumed that the catalyst volume scales proportionally with, and the space velocity inversely with, the bond dissociation energy of the reacting molecule. This assumption relies on the hypothesis that the catalytic efficiencies, expressed as the required catalyst volume per unit bond energy, are comparable between the TEP catalytic reactors (used for tritiated methane steam reforming) and the ISS equilibrators (used for converting the less stable hetero-isotopic molecules HD, HT, and DT into the preferred homo-isotopic forms H_2, D_2, and T_2).

The space velocity, expressed in $(Nm^3/h)/m^3_{catalyst}$), was taken from [52] and used to estimate the required catalyst volume for each equilibrator reactor. The corresponding reactor dimensions (diameter and height) were then derived assuming an L/D ratio between 2.5 and 5.0. The bond dissociation energies of hydrogen isotopologues were taken from [53].

The output of this step includes three key deliverables:

- **Product Specifications**, detailing the technical requirements for each component to guide vendor selection. An extract of the product specifications for the three cryogenic columns is reported in Table 5. Columns key parameters (diameter and packing height) are indicative and were extracted from the HYSYS database. For a more accurate size estimation, it is necessary to obtain validation from a column and packing vendor.
- **Process Flow Diagram (PFD)**, providing a comprehensive representation of process units, material flows, and system interconnections. It also includes auxiliary components such as pumps, heaters, and coolers to give a complete view of operational boundaries and integration.
- **Equipment List**, listing all the components identified in the PFD. For each component - named according to the project tagging procedure - the following information is provided: description, quantity, dimensions, capacity/duty, electric power, temperature (design/operating), pressure (design/operating), weight (empty/filled), notes, warnings/gap analysis, reference documents.

Together, these documents form the backbone for subsequent design stages, including for example layout definition, safety and asset integrity analyses, in compliance with the relevant code and standards.

Table 5
Example of the product specifications of the ISS cryogenic columns.

	Protium Enriched Column	Deuterium Enriched Column	Tritium Enriched Column
Theoretical stages [#]	123	96	66
Structured beds [#]	16	3	8
Height of the structured beds [mm]	440 (15 beds) 220 (1 bed)	1760 (3 beds)	495 (7 beds) 220 (1 bed)
Interspace [mm]	300	500	300
Estimated Diameter [m]	0.048	0.25	0.05
Estimated Packing Height [m]	~12	~ 6	~ 6

3.3.1. Tritium inventory estimation

A structured methodology has been developed to establish a consistent, transparent, and traceable framework for estimating tritium inventories across all TFC units. This approach is designed to ensure reliability and comparability of results, regardless of the level of detail or data availability for individual components.

The methodology is inherently flexible: it supports high-fidelity calculations when detailed operational data are available, while also enabling conservative bounding estimates in cases where only limited or preliminary information exists. This dual capability ensures that assessments remain robust throughout all stages of design maturity.

Furthermore, by standardizing the estimation process, the methodology facilitates uniform and comparable evaluations across different configurations and designs. This consistency is critical for informing design optimisation, safety analysis, and regulatory licensing decisions, ultimately contributing to a more rigorous and transparent decision-making process.

Being cryogenic and operating with liquid hydrogen, the ISS represents a significant contribution to the tritium inventory, requiring careful design to minimize safety risks and inventory hold-up. Inventory estimation was performed on:

- The three cryogenic distillation columns, including their condensers and reboilers stages. In particular, inventories within the reboiler were estimated considering a volume twice as big as a standard stage. The volume of each stage was calculated considering a pseudo-equivalent height given by the actual HETP plus the total interspace heights divided by the number of stages. Operative conditions (temperature, pressure, density, and composition) for each stage were extracted from the HYSYS® simulation and used for calculating the tritium amount within the columns. For each stage, a 10% volume of liquid and 90% volume of vapor have been considered in accordance with [51].
- The six equilibrator catalytic reactors, for which the entire volume was conservatively considered available for the process gas (i.e., neglecting the volume occupied by the catalyst material). The tritium concentration at the equilibrator feed was used to estimate the inventory. This assumption represents a balance between two competing effects: on one hand, the extremely high specific surface area of the catalyst (e.g., Pt nanoparticles) may lead to significant tritium adsorption, increasing the inventory; on the other hand, neglecting the physical volume of the catalyst and its support (e.g., metal particles and alumina or silica) tends to overestimate the available gas volume and thus partially compensates for this effect.
- The piping, whose volume was estimated assuming a total piping length of 49 m, made of eleven lines, of which five containing liquid phases and six containing gaseous phases, with diameters ranging from 5.48 mm (0.125″ type) to 7.66 mm (0.25″ type), schedule type 80S. An equivalent length factor of 1.1 was considered. No tritium was estimated in the piping walls, because of the extremely low temperature, effectively preventing tritium from diffusing into the metal.

Inventories in cryogenic pumps, reheaters, and coolers shown in the PFD were excluded from the preliminary estimations, given the complexity of accurately modelling cryogenic equipment at this stage of the study. To compensate for this simplification, a length factor of 2 was applied to all process lines, resulting in an intentional overestimation of the associated volumes.

Applying the assumption and methodologies discussed above, the tritium inventory for the ISS unit was estimated to be approximately 820 g. The distribution of this inventory across the main components is reported in Fig. 18.

3.4. Design verification and way forward

To complete the preliminary design phase, dynamic FC simulations are required to quantify material flows, inventory evolution, and system interactions under both normal and off-normal operating conditions. These simulations provide the basis for validating mass balance, identifying transient behaviours, and assessing compliance with safety margins. As a next step, layout segmentation will be defined in accordance with compliance and safety standards. This step involves establishing physical and functional zones aligned with international codes and regulations, such as ATEX for explosive atmospheres and OSHA for occupational safety. Radiological protection criteria, including dose-rate limits and confinement principles, will be integrated into the segmentation strategy to ensure defence-in-depth and regulatory conformity. Finally, asset integrity management procedures will be implemented for all fuel-cycle systems. These procedures encompass inspection protocols, preventive maintenance schedules, and lifecycle management of critical components. A risk-based methodology will be adopted to guarantee structural integrity and operational reliability under all conditions. All practices will be harmonized with industry best practices and

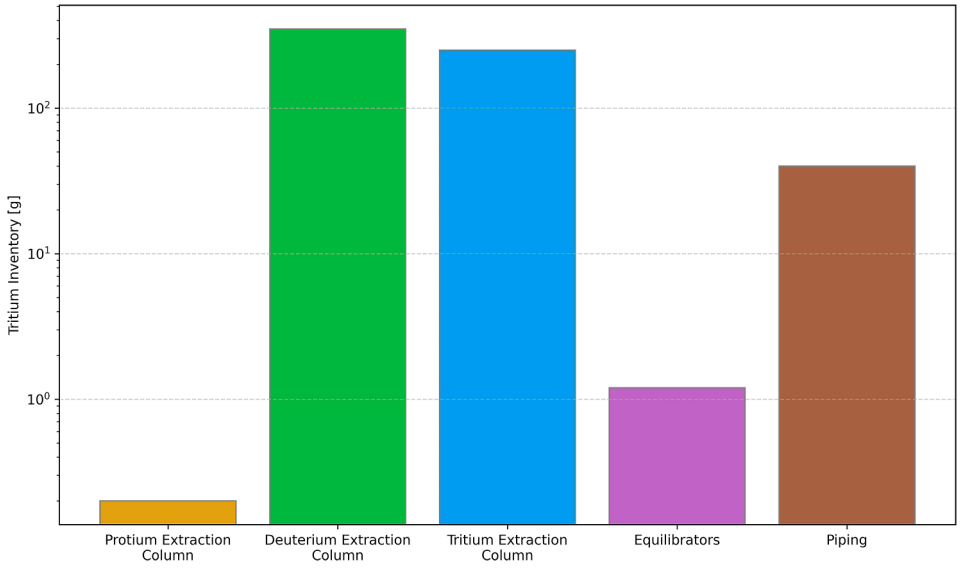

Fig. 18. Example of a breakdown of tritium inventories in ISS components.

applicable safety standards.

4. Conclusions

This study recommends the application of standardized engineering workflows and methodologies to accelerate the industrialisation of FPPs. By integrating traditional engineering activities such as multi-physics analyses, technology assessment and process simulations into a unified workflow, a structured approach is outlined suitable for preliminary design studies of Breeding Blanket and Tritium Fuel Cycle systems. In this framework, System Engineering principles, nuclear-grade design codes, and industrial manufacturing standards are pivotal in ensuring that design progresses in a structured and traceable way. The proposed workflow is conceived as an evolving structure: while it provides a consistent and repeatable baseline, it can be progressively refined as system-specific peculiarities emerge during early testing and application. Lessons learned at each iteration are systematically reincorporated, thereby enhancing workflow maturity and shortening development timelines.

The application of the methodology to the Breeding Blanket and Tritium Fuel Cycle systems provided concrete technical insights into its effectiveness. For the Breeding Blanket, the multi-physics parametric analyses enabled the identification of feasible design envelopes, such as minimum first-wall thicknesses, lithium enrichment levels, and coolant-channel configurations, capable of achieving TBR ≥ 1 while maintaining structural integrity and temperature limits. The thermal analyses also highlighted the influence of enhanced heat-transfer features (e.g., V-ribs) in reducing peak wall temperatures. For the Tritium Fuel Cycle, the structured process-design methodology led to a consistent preliminary architecture. The example of the Isotope Separation System demonstrated how the workflow guides the sizing of cryogenic distillation columns, equilibrators, and associated equipment. In addition, the introduction of a dedicated tritium-inventory estimation methodology supported early assessments of safety margins, regulatory considerations, and design optimisation.

These technical results reinforce the importance of early-stage process standardisation as a means to bridge the gap between experimental devices and commercially viable fusion power plants. By leveraging mature industrial practices, the proposed framework supports the transformation of scientific advances into deployable, reliable systems. Although the current analysis relies on preliminary assumptions that reflect the evolving status of fusion-plant development, the methodology is intentionally structured to incorporate increasing fidelity as improved data, physics models, and technological solutions become available.

Future work will build upon this initial stage by integrating dynamic simulations, applying risk-based design validation methodologies, and developing compliance-driven layout segmentation strategies. These analyses will allow operational reliability and regulatory conformity to be considered from the early stage of design, ultimately reinforcing the central statement of this work: *accelerating fusion energy through process standardisation*.

CRediT authorship contribution statement

G.V. Centomani: Writing – review & editing, Conceptualization. **A. Iaboni:** Writing – review & editing, Conceptualization. **D. Avella:** Writing – review & editing. **A. Buonocore:** Writing – review & editing. **L. Barone:** Writing – review & editing. **L. Cederle:** Writing – review & editing. **M. De Bastiani:** Writing – review & editing. **R. Durastanti:** Writing – review & editing. **G. Ferrero:** Writing – review & editing. **R. Forte:** Writing – review & editing. **E. Gallo:** Writing – review & editing. **D. Indrigo:** Writing – review & editing. **S. Meschini:** Writing – review & editing. **D. Pettinari:** Writing – review & editing. **F. Podenzani:** Writing – review & editing. **M. Romano:** Writing – review & editing. **D. Salvato:** Writing – review & editing. **R. Testoni:** Writing – review & editing. **M. Zucchetti:** Writing – review & editing. **G.A. Spagnuolo:** Writing – review & editing, Conceptualization.

Declaration of competing interest

The authors declare the following financial interests/personal relationships which may be considered as potential competing interests:

Alessandro Spagnuolo, given his role as editorial team of "Fusion Engineering and Design" journal, had no involvement in the peer review of this article and had no access to information regarding its peer review. Full responsibility for the editorial process for this article was delegated to another journal editor. If there are other authors, they declare that they have no known competing financial interests or personal relationships that could have appeared to influence the work reported in this paper.

Data availability

The data that has been used is confidential.

References

[1] A. Raffray, M. Akiba, L. Giancarli, V. Chuyanov, S. Malang, Breeding blanket concepts for fusion and materials requirements, J. Nucl. Mater. 307-311 (2002) 21–30, https://doi.org/10.1016/S0022-3115(02)01174-1.
[2] K. Hesch, L.V. Boccaccini, R. Stieglitz, Blankets - key element of a fusion reactor - functions, design and present state of development, Kerntechnik 83 (2018) 241–250, https://doi.org/10.3139/124.110923.
[3] AFCEN, Code of Design and Construction Rules For Mechanical Component in Nuclear Installations (RCC-MRX), 2022.
[4] D. De Meis, RCC-MRx Design Code For Nuclear Components, ENEA, 2015. RT/2015/28/ENEA.
[5] ISO, ISO/TC 85/SC 6 - Reactor technology, 1995.
[6] ISO, ISO/TC 85/SC 2 - Radiological Protection, 1980.
[7] ISO, ISO 16646:2024 Fusion installations — criteria for the Design and Operation of Confinement and Ventilation Systems of Tritium Fusion Facilities and Fusion Fuel Handling Facilities, 2024.
[8] R. Kembleton, C. Bustreo, Prospective research and development for fusion commercialisation, Fusion Eng. Des. 178 (2022) 113069, https://doi.org/10.1016/j.fusengdes.2022.113069.
[9] M. Coleman, S. McIntosh, BLUEPRINT: a novel approach to fusion reactor design, Fusion Eng. Des. 139 (2019) 26–38, https://doi.org/10.1016/j.fusengdes.2018.12.036.
[10] T. Davis, The need for codes and standards in nuclear fusion energy, J. Fusion Energy. 42 (2023), https://doi.org/10.1007/s10894-023-00350-2.
[11] G.A. Spagnuolo, Systems engineering approach in support to the breeding blanket design, Fusion Eng. Des. 146 (2019) 31–35, https://doi.org/10.1016/j.fusengdes.2018.11.016.
[12] G. Bongiovì, G.A. Spagnuolo, I.A. Maione, F. Cismondi, A. Del Nevo, F. Hernandez, D. Rapisarda, R. Mozzillo, Systems engineering activities supporting the heating & current drive and fuelling lines systems integration in the European DEMO breeding blanket, Fusion Eng. Des. 147 (2019) 111265, https://doi.org/10.1016/j.fusengdes.2019.111265.
[13] G. Bongiovì, P. Arena, P. Chiovaro, P.A. Di Maio, A. Del Nevo, R. Forte, Multi-module vs. Single-module concept: comparison of thermomechanical performances for the DEMO Water-cooled Lithium lead breeding blanket, Fusion Eng. Des. 136 (2018) 1472–1478, https://doi.org/10.1016/j.fusengdes.2018.05.037.
[14] M. Reith, M. Dürrschnabel, S. Bonk, U. Jäntsch, T. Bergfeldt, J. Hoffmann, S. Antusch, E. Simondon, M. Klimenkov, C. Bonnekoh, B.E. Ghidersa, H. Neuberger, J. Rey, C. Zeile, G. Pintsuk, G. Aiello, Technological processes for steel applications in nuclear fusion, Appl. Sci. 11 (2021) 11653, https://doi.org/10.3390/app112411653.
[15] M. Zmitko, European Test Blanket Modules: An Overview of Fabrication Technologies Development and Their Feasibility Assessment, in: IAEA TM on Tritium Breeding Blankets and Associated Neutronics, Vienna, 2025.
[16] Advanced Welding Processes for Fusion Reactor Fabrication - TWI, https://www.twi-global.com/technical-knowledge/published-papers/advanced-welding-processes-for-fusion-reactor-fabrication-september-1999.
[17] W. Wang, Standards Requirement And Development in Manufacturing of Water-Coolant Tritium Breeding Blanket Component, in: Technical Meeting on Experience in Codes and Standards for Fusion Technology, Vienna, 2025.
[18] ISO, ISO 16646:2024 Fusion installations — Criteria for the Design and Operation of Confinement and Ventilation Systems of Tritium Fusion Facilities and Fusion Fuel Handling Facilities, 2024.
[19] ISO, ISO/DIS 19991 - Fusion technology — Experimental magnetic confinement fusion facilities — Supersonic molecular beam injection fueling technique for fusion devices, 2025.

[20] ASME, BPVC.XI.2 - BPVC Section XI-Rules For Inservice Inspection of Nuclear Reactor Facility Components, Division 2, Requirements for Reliability and Integrity Management (RIM) Programs for Nuclear Reactor Facilities, 2025.
[21] F4E Fuel Cycle Technology Mapping Report, 2025. https://fusionforenergy.europa.eu/wp-content/uploads/2025/07/Fusion_Fuel_Cycle_Technology_Mapping_report_F4E_EUROfusion.pdf.
[22] S. Takeda, S. Ogawa, M. Tabuchi, Y. Kume, R. Pearson, C. Baus, S. Konishi, Kyoto Fusioneering UNITY Team, UNITY: kyoto Fusioneering's unique integrated testing facility for Fusion power generation, Fusion Sci. Technol. 79 (2023) 1059–1064, https://doi.org/10.1080/15361055.2023.2176689.
[23] C. Baus, H. Boniface, I. Castillo, A. Dashliborun, C. Day, T. Ino, M. Jimma, D. Kikuchi, M. King, S. Konishi, Y. Kume, S. Lee, N. Maki, Y. Matsunaga, J. McGrady, K. Namba, L. Neumann, Y. Nozoe, R. Pearson, D. Rynald, J. Schwenzer, S. Strickwerda, S. Suppiah, T. Teichmann, B. Uppal, T. Whitehorne, T. Yokoi, Conceptual design of UNITY-2, the fuel cycle test facility for Fusion pilot plants, Fusion Sci. Technol. 82 (2026) 357–372, https://doi.org/10.1080/15361055.2025.2481362.
[24] S. Liu, X. Ma, K. Jiang, X. Cheng, K. Huang, H. Neilsion, A. Khodak, P. Titus, Conceptual design of the water cooled ceramic breeder blanket for CFETR based on pressurized water cooled reactor technology, Fusion Eng. Des. 124 (2017) 865–870, https://doi.org/10.1016/j.fusengdes.2017.02.065.
[25] I. Fernández-Berceruelo, I. Palermo, F.R. Urgorri, D. Rapisarda, M. González, J. Alguacil, J.P. Catalán, J.M. García, J. Kekrt, M. Kordač, Progress in design and experimental activities for the development of an advanced breeding blanket, Nucl. Fusion 64 (2024) 056029, https://doi.org/10.1088/1741-4326/ad37ca.
[26] F. Cismondi, L.V. Boccaccini, G. Aiello, J. Aubert, C. Bachmann, T. Barrett, L. Barucca, E. Bubelis, S. Ciattaglia, A. Del Nevo, E. Diegele, M. Gasparotto, G. Di Gironimo, P.A. Di Maio, F. Hernandez, G. Federici, I. Fernández-Berceruelo, T. Franke, A. Froio, C. Gliss, J. Keep, A. Loving, E. Martelli, F. Maviglia, I. Moscato, R. Mozzillo, Y. Poitevin, D. Rapisarda, L. Savoldi, A. Tarallo, M. Utili, L. Vala, G. Veres, R. Zanino, Progress in EU breeding blanket design and integration, Fusion Eng. Des. 136 (2018) 782–792, https://doi.org/10.1016/j.fusengdes.2018.04.009.
[27] G. Federici, L. Boccaccini, F. Cismondi, M. Gasparotto, Y. Poitevin, I. Ricapito, An overview of the EU breeding blanket design strategy as an integral part of the DEMO design effort, Fusion Eng. Des. 141 (2019) 30–42, https://doi.org/10.1016/j.fusengdes.2019.01.141.
[28] J. Shimwell, R. Delaporte-Mathurin, J. Jaboulay, J. Aubert, C. Richardson, C. Bowman, A. Davis, A. Lahiff, J. Bernardi, S. Yasin, Multiphysics analysis with CAD-based parametric breeding blanket creation for rapid design iteration, Nucl. Fusion 59 (2019) 046019, https://doi.org/10.1088/1741-4326/ab0016.
[29] S. Merriman, J. Abraham, J. Bailey, J. Billingsley, B. Edwards, J. Hagues, D. L. Hernandez, N. Mantel, N. Otway, A. Saigiridhari, S. Sherwood, J. Ting, J. Fradera, P. Andres, A. Bernad, D. Catalan, S. Haouala, S. Sádaba, B. Echeveste, S. Ha, Integrated simulation for the preconceptual optioneering of the STEP breeder blanket design, Fusion Eng. Des. 189 (2023) 113423, https://doi.org/10.1016/j.fusengdes.2023.113423.
[30] P. Chiovaro, P.A. Di Maio, R. Favetti, G. Spagnuolo, A multi-physics integrated approach to breeding blanket modelling and design, Fusion Eng. Des. 143 (2019) 35–40, https://doi.org/10.1016/j.fusengdes.2019.03.131.
[31] Eni Internal Procedure (2026).
[32] B. Sorbom, J. Ball, T.R. Palmer, F.J. Mangiarrotti, J.M. Sierchio, P. Bonoli, C. Kasten, D.A. Sutherland, H.S. Barnard, C.B. Haakonsen, J. Goh, C. Sung, D. G. Whyte, ARC: a compact, high-field, fusion nuclear science facility anddemonstration power plant with demountable magnets, Fusion Eng. Des. (2015), https://doi.org/10.1016/j.fusengdes.2015.07.008.
[33] A.Q. Kuang, N.M. Cao, A.J. Creely, C.A. Dennett, J. Hecla, B. LaBombard, R. A. Tinguely, E.A. Tolman, H. Hoffman, M. Major, J. Ruiz Ruiz, D. Brunner, P. Grover, C. Laughman, B. Sorbom, D. Whyte, Conceptual design sttudy for heat exhaust management in the ARC fusion pilot plant, Fusion Eng. Des. 137 (2018) 221–242, https://doi.org/10.1016/j.fusengdes.2018.09.007.
[34] S. Segantin, Z. Hartwig, D.G. Whyte, M. Zucchetti, Exploration of a fast pathway to nuclear fusion: thermal analysis and cooling design considerations for the ARC reactor, Fusion Sci. Technol. 76 (2020) 45–52, https://doi.org/10.1080/15361055.2019.1629252.
[35] S. Segantin, R. Testoni, M. Zucchetti, Neutronic comparison of liquid breeders for ARC-like reactor blankets, Fusion Eng. Des. 160 (2020) 112013, https://doi.org/10.1016/j.fusengdes.2020.112013.
[36] J.W. Bae, D. Young, K. Borowiec, V. Badalassi, Integral analysis of the effect of material dimension and composition on tokamak neutronics, Nucl. Fusion 64 (2024) 056013, https://doi.org/10.1088/1741-4326/ad33ee.
[37] https://openmc.org/.
[38] https://www.nndc.bnl.gov/endf-b8.0/.
[39] F. Ledda, D. Pettinari, G. Ferrero, F. Laviano, S. Meschini, S. Sparacio, R. Testoni, D. Torsello, M. Zucchetti, 3D neutronic analysis on compact fusion reactors: pHITS-OpenMC cross-comparison, Fusion Eng. Des. 202 (2024) 114323, https://doi.org/10.1016/j.fusengdes.2024.114323.
[40] G. Ferrero, R. Testoni, S. Meschini, M. Zucchetti, Exploration of ARC-class reactor vessel and divertor cooling system, Fusion Eng. Des. 192 (2023) 113818, https://doi.org/10.1016/j.fusengdes.2023.113818.
[41] Ansys 2023/R2 Take A Leap Of Certainty (TM). Command Reference, Canonsburg, PA 15317, 2023.
[42] L. Shere, A.K. Hill, T.J. Mays, R. Lawless, R. Brown, S.P. Perera, The next generation of low tritium hydrogen isotope separation technologies for future fusion power plants, Int. J. Hydrog. Energy 55 (2024) 319–338.
[43] M. Inoue, S. Konishi, T. Yamanishi, S. Ohira, T. Watanabe, K. Okuno, Y. Naruse, R. H. Sherman, J.W. Barnes, J.R. Bartlit, J.L. Anderson, Isotope separation system experiments at the TSTA, Fusion Technol. 21 (1992) 293–298, https://doi.org/10.13182/FST92-A29760.
[44] N. Bainbridge, A.C. Bell, P.D. Brennan, S. Knipe, R. Lässer, R. Stagg, Operational experience with the JET AGHS cryodistillation system during and after DTE1, Fusion Eng. Des. 47 (1999) 321–332, https://doi.org/10.1016/S0920-3796(99)00089-7.
[45] J.R. Robins, K.B. Woodall, G. Woo, D.G. Bellamy, S.K. Sood, C. Fong, Tritium Purification System for TFTR, in: 15th IEEE/NPSS Symposium Fusion Engineering, 2024, https://doi.org/10.1109/FUSION.1993.518285.
[46] I. Cristescu, I.R. Cristescu, L. Dörr, M. Glugla, G. Hellriegel, R. Michling, D. Murdoch, P. Schäfer, S. Welte, W. Wurster, Commissioning of water detritiation and cryogenic distillation systems at TLK in view of ITER design, Fusion Eng. Des. 82 (2007) 2126–2132, https://doi.org/10.1016/j.fusengdes.2007.04.001.
[47] M. Lord, I. Bennet, C. Harrington, A. Cooper, D. Lee-Lane, A. Cureton, C. Olde, M. Thompson, D. Jayasundara, T. Meatyard, Fusing together an outline design for sustained fuelling and tritium self-sufficiency, Phil. Trans. R. Soc. A. 382 (2024), https://doi.org/10.1098/rsta.2023.0410.
[48] L. Shere, A.K. Hill, T.J. Mays, R. Lawless, R. Brown, S.P. Parera, The next generation of low tritium hydrogen isotope separation technologies for future fusion power plants, Int. J. Hydrog. Energy 55 (2024) 319–338, https://doi.org/10.1016/j.ijhydene.2023.10.282.
[49] AspenTech Website, https://www.aspentech.com/en/products/engineering/aspen-hysys.
[50] E. Iraola, J.M. Nougués, L. Sedano, J.A. Feliu, L. Batet, Dynamic simulation tools for isotopic separation system modeling and design, Fusion Eng. Des. 169 (2021) 112452, https://doi.org/10.1016/j.fusengdes.2021.112452.
[51] J.C. Schwenzer, C. Day, T. Giegerich, A. Santucci, Operational tritium inventories in the EU-DEMO fuel cycle, Fusion Sci. Technol. 78 (2022) 664–675, https://doi.org/10.1080/15361055.2022.2101834.
[52] Y. Edao, Y. Iwai, Decomposition of methane with various precious metal catalysts for the tokamak exhaust processing, Fusion Eng. Des. 171 (2021) 112685, https://doi.org/10.1016/j.fusengdes.2021.112685.
[53] S. Leung, D. Hibbitts, M. Gárcia-Diéguez, E. Iglesia, Binding and exchange reactions of hydrogen isotopes on surfaces of dispersed Pt nanoparticles, J. Phys. Chem. 126 (2022) 3923–3938, https://doi.org/10.1021/acs.jpcc.1c09131.